

5 APPENDIX

5.1 DENSITY POROSITY FORMULA

In order to be able to compute loads, we need information about the density of the sediments. Under normal conditions one can accept a constant density. But in applying for example in south China sea (BRAITENBERG ET AL. 2005) the problem resulted that the sediments reach up to a depth of $d = 12km$. Here we can not assume a constant density. The density of the sediments increases with the depth. If it concerns oceanic sediments, then the concept of porosity plays an important role. Therefore in the following we will construct a formula taking porosity and density information from boreholes into account.

Large extended sediment basins produce a long-wave gravity signal. This has an important influence on the calculation of the CMI depth variation. Therefore, it is necessary to determine first the gravity effect of the sediment basin and reduce this effect from the gravity signal. To compute the gravity effect the densities of the sediments are required. The density of the sediments increases with depth. Since porosity is also a function of depth, one can construct a formula to calculate the density of sediments (application in Chapter 3.1) by using the porosity. The general porosity formula is (e.g. SU ET AL. 1989) :

$$\Phi = \Phi_0 \cdot e^{-b \cdot d} \quad (5.1.1)$$

thereby is Φ the porosity, d the depth and Φ_0 is the initial porosity of the sediments at the surface. The parameter b must be determined by calibration, e.g. from boreholes. The bulk density of a rock is composed of the density of the fluid ρ_f and the grain density ρ_s which is related to the porosity by:

$$\rho = \Phi \cdot \rho_f + (1 - \Phi) \cdot \rho_s \quad (5.1.2)$$

For example in South China Sea we can assume $\rho_f = 1050kg/m^3$ and $\rho_s = 2700kg/m^3$. Using Eq. 5.1.1 and 5.1.2, a general density porosity formula results:

$$\rho(d) = \Phi_0 \cdot e^{-b_1 \cdot d} \cdot \rho_f + (1 - \Phi_0 \cdot e^{-b_2 \cdot d}) \cdot \rho_s \quad (5.1.3)$$

As boundary conditions in e.g. South China Sea we have porosity/depth data of IODP Leg 184. Therefore results the idea to use the density values from borehole measurements - shown in Table 5.1.1. and to construct a new function. In the following the density values are used for construction of a depth-density function. If we would fit the data with a linear relation, then we would overestimate the density value for sediments at a depth $d = 10km$. This means, that we would create a pseudo anomaly in large depth. Therefore is it essential to find a function in such way, that it approximates at greater depth a constant value, e.g. $\rho_s = 2800kg/m^3$. For the radical - logarithm function we observe a good fit with the data.

However, the exponential function is physically better explained and for this reason this function is favored (see Fig. 5.1.2).

depth [m]	name of boreholes						density [kg/m ³]
	Site 1148		Site 1143		Site 1144B		
	min	max	min	max	min	max	
100	1570	1650	1450	1600	1500	1600	
200	1650	1700	1500	1700	-	-	
300	-	-	1520	1700	1650	1700	
400	-	-	1600	1750	-	-	
500	-	-	-	-	1800	1900	

Table 5.1.1) minimal and maximal density values from borehole measurements

The exponential function is described by the following equation:

$$\rho(z) = 0.8 \cdot e^{-0.44z} \cdot 1.04 + (1 - 0.8 \cdot e^{-0.44z}) \cdot 2.8 \quad (5.1.4)$$

By comparison of Eq. 1.4.4 with Eq. 1.4.3 we conclude 0.8 for the initial porosity. This fits to the results from borehole measurements 80%. The data adjustment gives the density of the fluid with $\rho_f = 1040 \text{ kg/m}^3$. This is comparable with borehole measurement of $\rho_f = 1050 \text{ kg/m}^3$. The grain density is through the data adjustment $\rho_s = 2800 \text{ kg/m}^3$. According to the borehole measurements a density value of $\rho_s = 2700 \text{ kg/m}^3$ is obtained.

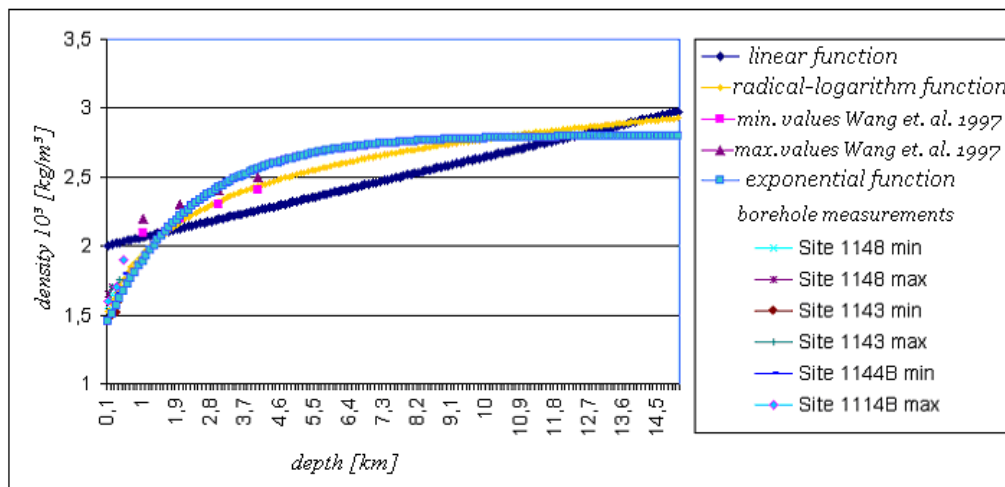


Figure 5.1.2) Construction of a depth-density function using information from borehole measurements. A linear relation could not be found (see dark blue colored Graph). The radical - logarithm function has a good fit to the data (yellow color). However, the exponential function (light blue color) is better explained in the physical way.

In order to avoid producing a pseudo gravity anomaly at greater depth, it is better to use the value $\rho_s = 2800\text{kg}/\text{m}^3$, since the exponential function converges to this density value in the infinite (if d becomes infinitely large) and this density value fits also to the density value of the reference crust. The parameter b was determined with $b = 0.44$. This function was insert into the slice program, which was introduced in the Chapter 1.4.

5.2 COMPARISON OF FLEXURE CURVES

5.2.1 FFT solution compared with logarithm and sine function

In Chapter 2.5, the flexure curves calculated with the analytical solution are compared with the flexure curves derived by FFT methods. The following Figs. 5.2.1 to 5.2.4 illustrate the agreement of the flexure curves for a specific T_e value and a certain factor.

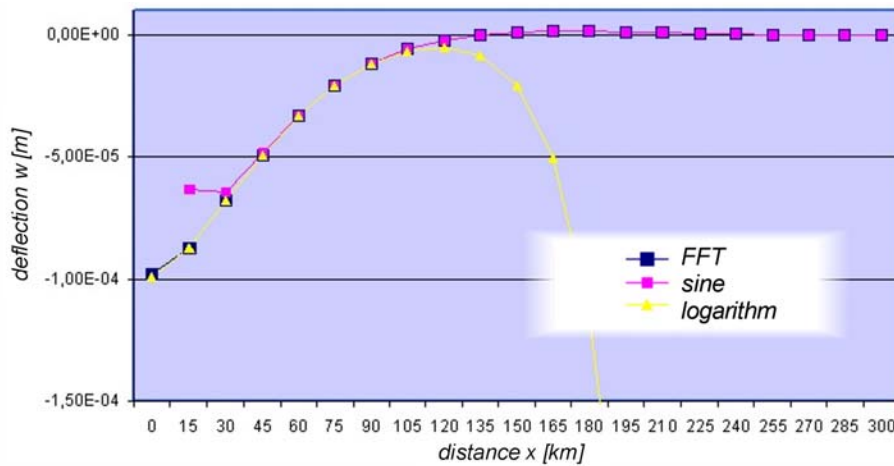


Figure 5.2.1) Comparison of flexure curve calculated for $T_e = 10\text{km}$. The flexure curve fits for a factor $fact = 2.25 \cdot 10^5$.

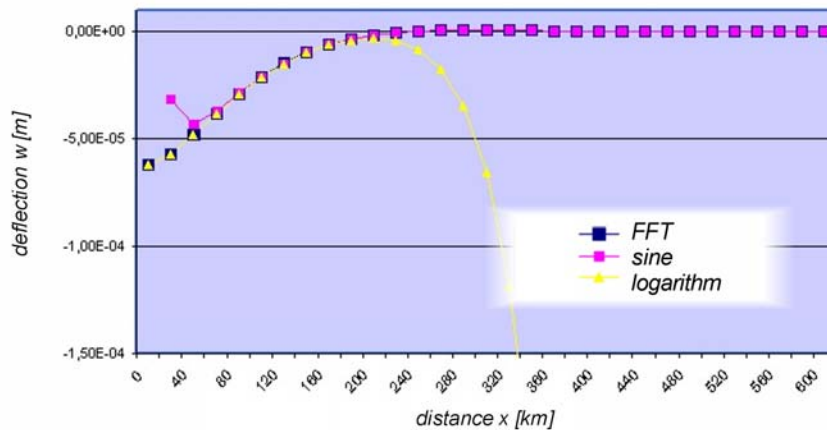


Figure 5.2.2) Comparison of flexure curve calculated for $T_e = 20\text{km}$. The flexure curve fits for a factor $fact = 4 \cdot 10^5$.

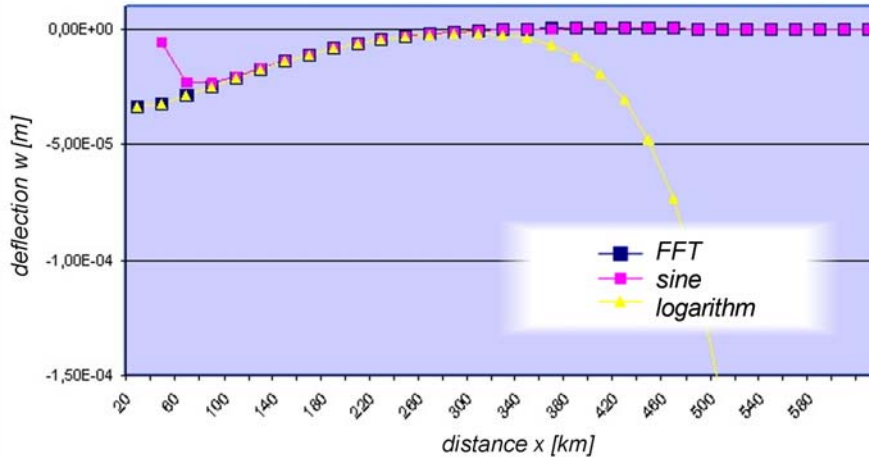


Figure 5.2.3) Comparison of flexure curve calculated for $T_e = 30km$. The flexure curve fits for a factor $fact = 4 \cdot 10^5$.

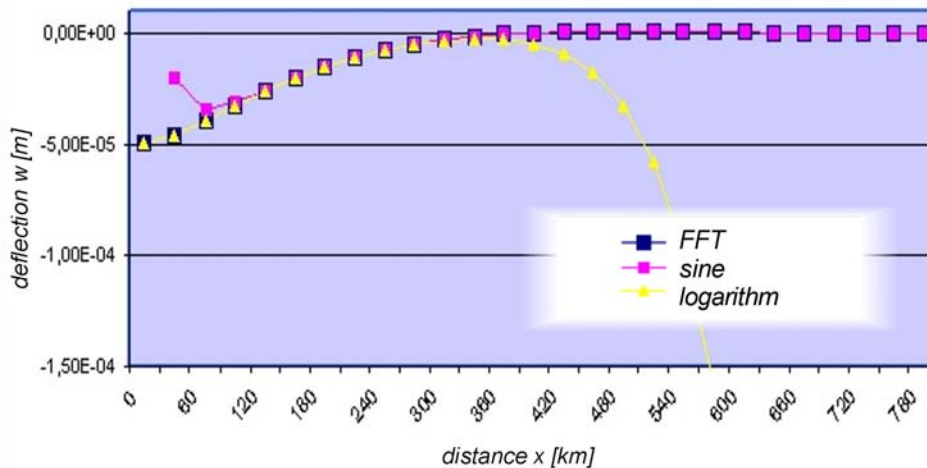


Figure 5.2.4) Comparison of flexure curve calculated for $T_e = 40km$. The flexure curve fits for a factor of $fact = 9 \cdot 10^5$.

5.2.2 Comparison of output from computer program with FFT

As mentioned at the end of Chapter 2.5.2, the output of the computer program has been compared with the flexure curves of the analytical solution and derived from the FFT methods. We obtain a very good agreement between all functions. In Figs. 5.2.5 to 5.2.7 the deflection curves in $[m/km]$ over a distance x calculated for $T_e = 5km$ are shown. Thereby the logarithm function is colored dark blue, the sinus function light blue, the output flexure of the Fortran computer program red and the flexure curves derived from FFT methods orange. Enlarging the graph, we obtain the "automatically switch" of the computer program from the logarithm function to the sinus function. Obviously, at close range the curve from the computer program (red) agrees with the logarithm function (dark blue) in the wide range with the sinus function (light blue). The flexure curve computed by the software fits well to

the flexure curves derived with FFT methods (orange). For further enlarging of the graph we obtain as well a very good agreement of all functions for the bulge.

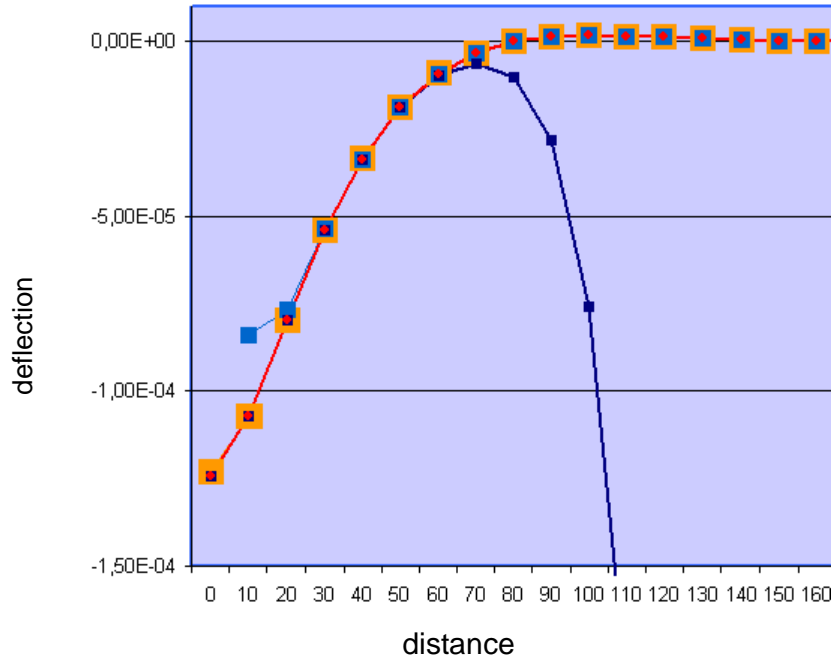


Figure 5.2.5) The flexure curves were calculated for $T_e = 5km$. The deflection in $[m/km]$ of the logarithm function is dark blue, the sine function light blue, the output of the computer program is red and derived from FFT methods are orange colored.

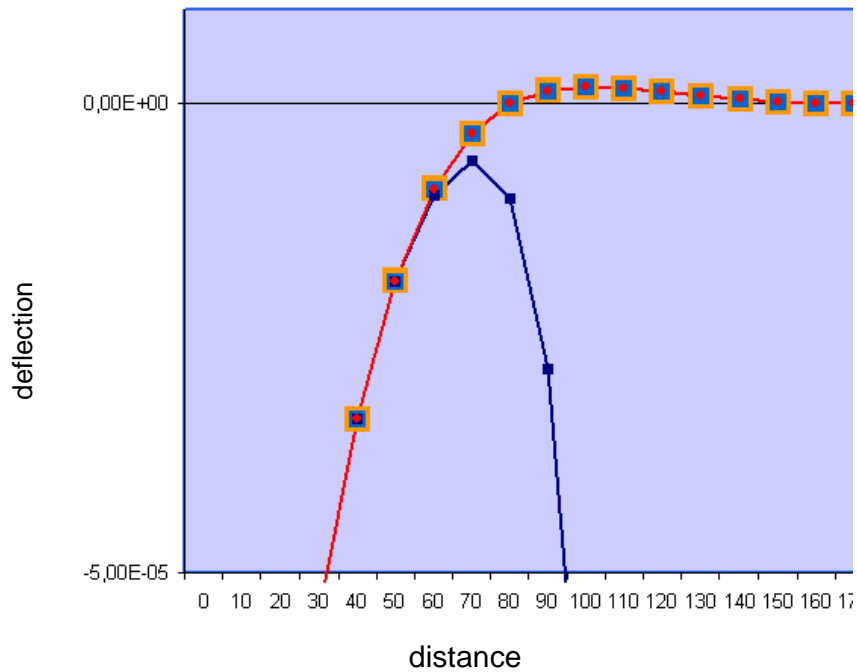


Figure 5.2.6) Zoom of Figure 5.2.5 shows the deflection in $[m/km]$ calculated for $T_e = 5km$ for the logarithm function (dark blue), the sine function (light blue), the output of the computer program (red) and from FFT (orange).

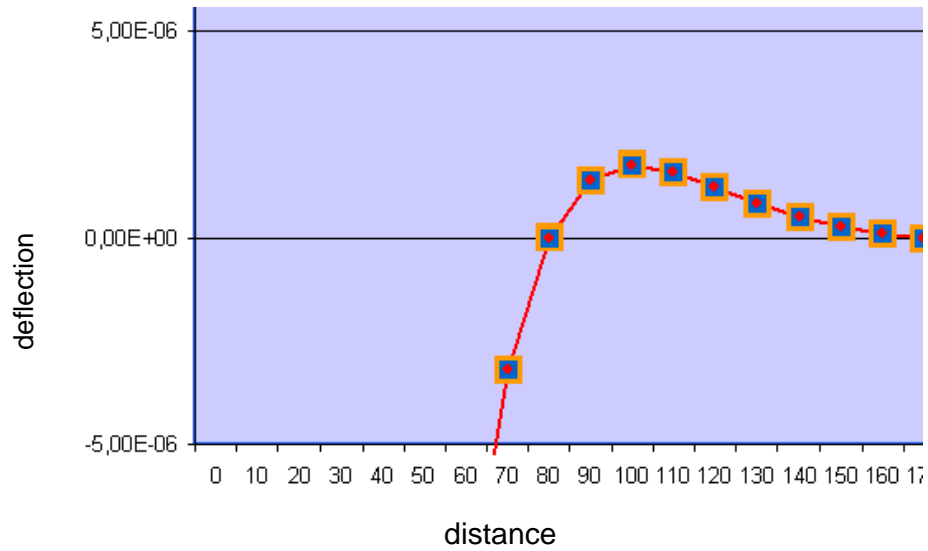


Figure 5.2.7) Further zoom of Figure 5.2.5 shows the bulge of the deflection in $[m/km]$ calculated for $T_e = 5km$.

5.3 FE MODELS

5.3.1 Calculation input parameters and results

Name of FEmodel	P_z [Pa]	F bzw. F_{min} / F_{max} [N]	E_1 / E_2 [Pa]	g [m/s^2]	time [s]	Steps	max. iterations	y-displacement [m]
susi_1	10^3		$10^{13} / 10^{13}$	-9.81	1.0	22	40	-94096.73
susi_2	6×10^8		$10^{13} / 10^{13}$	-9.81	1.0	22	40	-75862.35
susi_3	6×10^9		$10^{13} / 10^{13}$	-9.81	1.0	22	40	+802088.20
susi_4	10^9		$10^{13} / 10^{13}$	-9.81	1.0	22	40	-292.10
susi_5	1.1×10^9		$10^{13} / 10^{13}$	-9.81	1.0	22	40	+214.24
susi_6	1.05×10^9		$10^{13} / 10^{13}$	-9.81	1.0	22	40	+4.28
susi_7	1.05×10^9		$10^{12} / 10^{12}$	-9.81	1.0	22	40	+50.70
susi_8	1.05×10^9		$10^{11} / 10^{11}$	-9.81	1.0	22	40	+118269.90
susi_9	1.03×10^9		$10^{12} / 10^{12}$	-9.81	1.0	22	40	-412.85
susi_11	1.05×10^9		$10^{12} / 10^{12}$	-10.0	1.0	22	40	-420.33
susi_12	1.07×10^9		$10^{12} / 10^{12}$	-10.0	1.0	22	40	+46.08
susi_13		-10^4	$10^{12} / 10^{12}$	-10.0	1.0	22	40	-15.02
susi_14		-10^4	$10^{12} / 10^{12}$	without	1.0	22	40	-3.14×10^{-8}
susi_15		-10^4	$10^{10} / 10^{10}$	without	1.0	22	40	-3.14×10^{-6}
susi_16		-10^5	$10^{10} / 10^{10}$	without	1.0	22	40	-3.14×10^{-5}
susi_17		-10^6	$10^{10} / 10^{10}$	without	1.0	22	40	-3.14×10^{-4}
susi_18		-10^8	$10^{10} / 10^{10}$	without	1.0	22	40	-3.14×10^{-2}
susi_19		-10^{12}	$10^{10} / 10^{10}$	without	1.0	22	40	-339.43
susi_20		-10^{12}	$10^{12} / 10^{12}$	without	1.0	22	40	-3.41
susi_21		-10^{12}	$10^{10} / 10^{12}$	without	1.0	22	40	-266.96
susi_22		-10^{12}	$10^{10} / 10^{12}$	-10.0	1.0	22	40	-598.48
susi_23		-10^{12}	$10^{10} / 10^{10}$	-10.0	1.0	22	40	-1724.01

susi_24		-10^{10}	$10^{10} / 10^{12}$	without	1.0	22	40	-5.35
susi_25		-10^{12}	$10^{10} / 10^{12}$	without	1.0	22	40	-7569.98
susi_26		-10^{12}	$10^{10} / 10^{13}$	without	1.0	22	40	-1255.87
susi_27		-10^{12}	$10^{10} / 10^{11}$	without	1.0	22	40	-58123.76
susi_28		-10^{12}	$10^{12} / 10^{12}$	without	1.0	22	40	-1006.14
susi_29	vgl. susi_26	-10^{12}	$10^{10} / 10^{13}$	without	1.0	22	40	-1266.11
susi_30		-10^{12}	$10^{10} / 10^{13}$	without	100.0	22	40	-1266.11
susi_31		-10^{12}	$10^{10} / 10^{13}$	without	100.0	200	40	-3407.00
susi_32		-10^{12}	$10^{10} / 10^{13}$	without	100.0	500	40	-6017.04
susi_33		-10^{12}	$10^{10} / 10^{13}$	without	1000.0	500	40	-6025.17
susi_34		-10^{12}	$10^{10} / 10^{13}$	without	100.0	1	40	-1064.92
susi_35		-10^{12}	$10^{10} / 10^{13}$	without	100.0	1000	40	-10000.33
susi_36		-10^4	$10^{10} / 10^{13}$	without	100.0	1	40	-2.25×10^{-6}
susi_37		-10^4	$10^{10} / 10^{13}$	without	100.0	10	40	-2.68×10^{-6}
susi_38		-10^4	$10^{10} / 10^{13}$	without	100.0	100	40	-2.75×10^{-6}
susi_39		-10^4	$10^{10} / 10^{13}$	without	100.0	1000	40	-2.76×10^{-6}
susi_40		-10^4	$10^{10} / 10^{13}$	without	100.0	10000	40	-2.76×10^{-6}
susi_41		-10^9	$10^{10} / 10^{13}$	without	100.0	100	50	-0.27
susi_42		-10^9	$10^{10} / 10^{13}$	without	100.0	200	50	-0.27
susi_43		-10^9	$10^{10} / 10^{13}$	without	100.0	200	50	-0.27
susi_44		-10^{10}	$10^{10} / 10^{13}$	without	100.0	100	50	-2.75
susi_45		-10^{11}	$10^{10} / 10^{13}$	without	100.0	100	50	-29.28
susi_46		-2×10^{11}	$10^{10} / 10^{13}$	without	100.0	100	50	-76.53

The following FE models are calculated without gravity.

name	l_F [km]	F bzw. F_{\max} / F_{\min} [N]	E_1 / E_2 [Pa]	time [s]	Steps	max. iterations	y- displacement [m]
susi_47	120	-10^{10}	$10^{10} / 10^{13}$	100.0	100	50	-27.11
susi_48	240	-10^{10}	$10^{10} / 10^{13}$	100.0	100	50	-42.13
susi_49	60	-10^{10}	$10^{10} / 10^{13}$	100.0	100	50	-7.67
susi_50	120	$-10^{10} / -10^7$	$10^{10} / 10^{13}$	100.0	100	50	-6.78
susi_51	120	$-10^{10} / -10^8$	$10^{10} / 10^{13}$	100.0	100	50	-6.84
susi_52	192	$-10^{10} / -4 \times 10^8$	$10^{10} / 10^{13}$	100.0	100	50	-12.69
susi_53	192 _p	$-10^{11} / 0$	$10^{10} / 10^{13}$	100.0	100	50	-38.36
susi_54	120	$-10^{10} / -10^8$	$10^{10} / 10^{13}$	100.0	100	50	-51.54
susi_55	60	central - $10^{10} / -10^8$	$10^{10} / 10^{13}$	100.0	100	50	-4.18
susi_56	60	central - $5 \times 10^{10} / -5 \times 10^8$	$10^{10} / 10^{13}$	100.0	100	50	-46.00
susi_57	60	right - $5 \times 10^{10} / -5 \times 10^8$	$10^{10} / 10^{13}$	100.0	100	50	-48.11

The following models are calculated without gravity, time=100s, 100 steps, and with maximum 50 iterations.

	F bzw. F_{\max} / F_{\min} [N]	E_1 / E_2 [Pa]	C_1 / C_2 [Pa]	ϕ_1 / ϕ_2 [°]	$\sigma_{y1} / \sigma_{y2}$ [Pa]	
susi_58	right $-5 \times 10^{10} / -5 \times 10^8$	$10^{10} / 10^{13}$	$2 \times 10^{10} / 2 \times 10^7$	31 / 31		-48.12
susi_59	-5×10^{10}	$10^{10} / 10^{13}$	$2 \times 10^{10} / 2 \times 10^7$	31 / 31		-13.88
susi_60	-5×10^{10}	$10^{10} / 10^{13}$	$2 \times 10^7 / 2 \times 10^7$	31 / 31		-13.88
susi_61	-5×10^{10}	$10^{10} / 10^{13}$	$2 \times 10^{10} / 2 \times 10^{10}$	31 / 31		-13.79
susi_62	-5×10^{10}	$10^{11} / 10^{13}$	$2 \times 10^{10} / 2 \times 10^{10}$	31 / 31		-2.70
susi_63	-5×10^{10}	$10^{10} / 10^{13}$	$2 \times 10^{10} / 2 \times 10^{10}$	15 / 31		-13.79
susi_64	-5×10^{10}	$10^{10} / 10^{13}$	$2 \times 10^{10} / 2 \times 10^{10}$	40 / 40		-13.79
susi_65	-5×10^{10}	$10^{10} / 10^{13}$			$10^7 / 10^8$	-13.79
susi_66	-5×10^{10}	$10^{10} / 10^{13}$			$10^7 / 10^8$	-13.79
susi_67	-5×10^{10}	$10^{10} / 10^{13}$			$10^7 / 10^7$	-21.08

5.3.2 Settings of the FE models

